XIII ICSMFE, 1994, New Delhi, India / XIII CIMSTF, 1994, New Delhi, Inde

STIFFNESS OF CARBONATIC QUIOU SAND

RIGIDITE DU SABLE CARBONATIQUE DE QUIOU

V. Fioravante[1] *M. Jamiolkowski*[2] *D.C.F. Lo Presti*[2]

[1]ISMES, Bergamo, Italy
[2]Politecnico di Torino, Italy

SYNOPSIS

The stiffness of the carbonatic uncemented Quiou sand was measured in laboratory on dry and saturated reconstituted samples by means of Resonant Column, Triaxial and Bender Element tests. Particular attention was devoted to the stiffness at very small (< 10^{-3} %) and at intermediate strain level (from 10^{-3} % to 0.5 %). The laboratory apparatuses and the testing procedures are briefly described; typical examples of the obtained results are presented. Assuming isotropic elasticity, the experimental data were analysed in terms of maximum shear modulus as a function of the state parameters and the results of the different tests were compared. Finally, the effects of the overconsolidation on the stiffness are examined, together with some considerations on modelling the stress-strain response by the hyperbolic model.

INTRODUCTION

Preliminary results of a series of laboratory tests performed on specimens of dry and saturated carbonatic Quiou sand (QS), are presented. The testing program includes Resonant Column test (RC) on dry samples, drained Triaxial Compression test (TX) on saturated samples, and measurement of shear wave velocity by means of piezoelectrical transducers, called Bender Elements (BE), on both dry and saturated soil samples.

Both RC and TX specimens have been subjected to isotropic consolidation in the range of stress varying between 100 to 600 kPa. While the TX and RC tests allow to explore a wide range of strains, the BE, incorporated on the triaxial cell, enables to measure the shear wave velocity and therefore the shear modulus, only at very small strains (i.e. about 10^{-4} %).

The above mentioned laboratory tests are part of a more extensive research effort involving the validation of different in situ devices in crushable and slightly silty sand using the calibration chambers and using numerical modelling (Almeida et al. 1991, Baldi et al. 1991, Bellotti et al. 1982, 1988, 1991).

Because of length constraint, the proceeding presentation is limited to the exam of the measurements of the shear stiffness at very small (< 10^{-3} %) and intermediate strain level (from 10^{-3} % to 0.5 %).

LABORATORY APPARATUSES

The triaxial testing system used for the tests, consists in a stress path triaxial cell with internal tie roads completely controlled by a personal computer. The cell has an internal load cell to measure the axial load without any piston friction. For some of the tests finalised to the determination of stiffness at very small strain, a load cell of 0.5 kN with an accuracy of 0.5 % of the measuring range, was adopted. This means an accuracy of 0.06 kPa in measuring axial stress.

The loading piston can be connected to the sample cap before assembling the pressure cell, therefore some of the bending errors can be avoided or reduced (such as the load and sample alignment). Nevertheless, in order to avoid vertical compliance of the triaxial apparatus, which involves the deformation of the load cell, the vertical and radial deformations of the sample are measured locally by means of the proximity transducers; this allows more reliable Poisson's ratio values, at least at small strains.

The used system of six proximities hanged on two bars, is schematised in figure 1: four out of them are fixed vertically to measure axial strains while two are fixed horizontally to measure the radial strains at the middle height of the sample. The proximity transducers used have a maximum measuring range of 2.5 mm; the resolution (<0.3 microns) and the accuracy (= 0.3 microns) were obtained from a calibration by a laser interferometer. The vertical targets, supported by pins, are inserted into the specimen and sealed to the membrane, while the horizontal ones are stuck on the membrane.

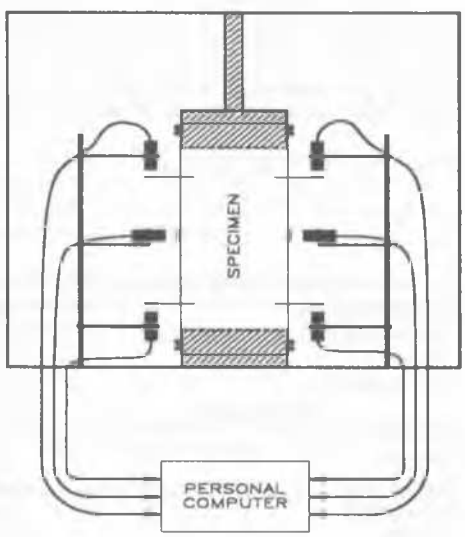

Figure 1 - Local measurements of axial and radial displacements by proximity transducer.

For the data logging acquisition, an analogical to digital converter of 16 bit was employed capable of reading 40 channels per second. In order to maximise the amplification of the proximities and the loading cell output signals, an analogue recorder was adopted in parallel, only for the first part of the shearing stage.

The triaxial cap and pedestal were instrumented with piezoelectrical transducers called Bender Elements (BE). When a driving voltage is applied to one of the elements, it bends to one side generating a shear wave that propagates along the sample; the other element, which acts as a receiver, converts the deflection due to the particle motion into an electrical signal and thus detects the arrival of the shear wave at the other end of the sample. The test result consists of the measure of the travel time from which the shear wave velocity (V_S) is calculated and, assuming isotropic elasticity, the shear modulus is $G = \rho V_S^2$ (for details see Brignoli and Gotti 1991).

A fixed-free Resonant Column apparatus was used for solid cylindrical dry specimens, consolidated isotropically. Since the apparatus is well known, details are neglected. Volume and height variations were measured during consolidation steps and dynamic shearing phases.

TEST SAND AND TESTING PROCEDURES

The physical properties of QS are summarised in figure 2. It is a sub angular well graded, coarse to medium sand, containing about 2 % of fines, as shown in figure 2, where are also indicated the minimum (obtained by pluviation) and the maximum (ASTM D4 254-83) unit weight and the correspondent void ratios.

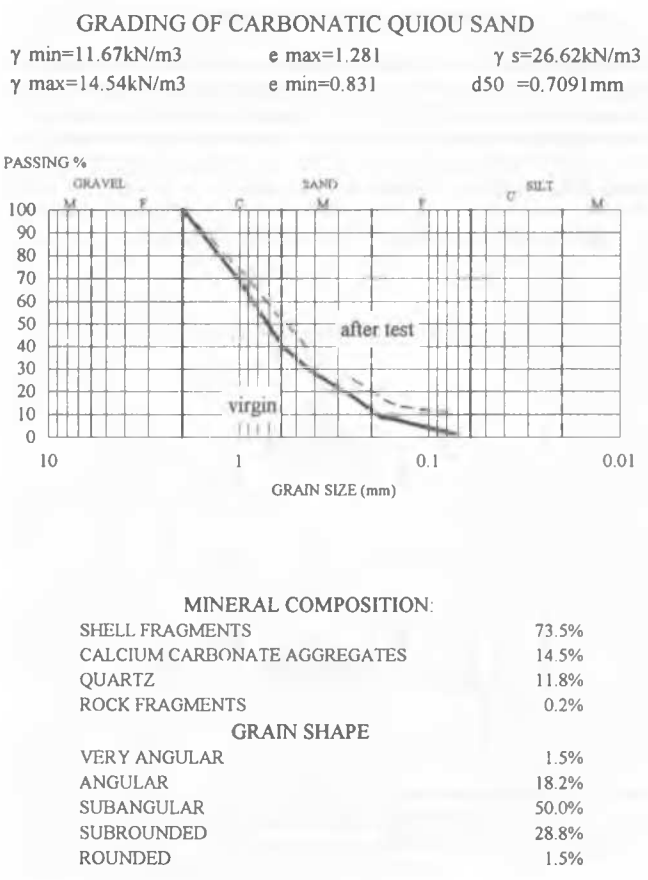

Figure 2 - Physical properties of Quiou Sand.

A high degree of crushability, even at small compressing or shearing stresses, is its peculiarity, which causes a continuous relevant change of void ratio, grain size distribution and grain morphology during the tests; the grain size distribution after TX testing is also shown in figure 2.

The specimens of 70 mm in diameter and 140 mm in height, were reconstituted by pluvial deposition using a travelling sand spreader (Passalacqua 1991). Only for some RC tests smaller samples were tested (i.e. 50 mm in diameter and 110 mm in height).

The tests, whose results are being presented, were isotropically consolidated within the range of stress varying from 100 to 600 kPa; after the consolidation, 12 hour's rest was observed to allow a significant stabilisation of strains. The BE tests were performed at the end of the rest period.

The shearing stage of the TX tests was carried out in drained conditions, under a strain controlled frame, at a constant rate of axial strain (about 10-4 % per second). The radial pressure was kept constant or adjusted in order to keep constant the mean effective stress (p').
For dry samples (RC and some BE tests) the current void ratio was evaluated from the volume changes measured by a special device capable to measure the air volume changes.

TEST RESULTS

A first part of a typical stress-strain relationship obtained from a TX test (CID304P), is reported in figure 3, where the deviatoric stress is plotted against the deviatoric shear strain. The experimental data are fitted by small segments, whose slope is taken as tangent modulus. The shear modulus so evaluated is also shown in figure 3 versus the correspondent shear strain.

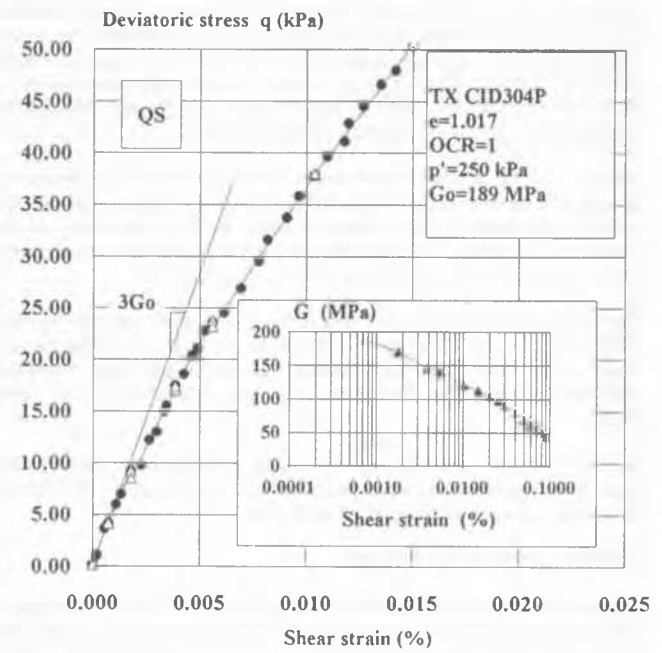

Figure 3 - A stress-strain relation at small strain in a TX test.

A typical trend of the Poisson's ratio versus the axial strain, is shown in figure 4. No substantial differences can be noted between the strains locally measured and those derived by mean of the external measures of the axial strain and the volume changes. It is important to note that the v values start at

0.27 at very small strain then decreases to 0.1 at ε_a = 0.5 %; successively increases for large strains. Such behaviour, usually notes in the tests so far performed can be ascribed to the crushability and the consequent rearrangement of the particles of the QS which increases as the strain increases up to a certain value (e.g. 0.5 %). Furthermore, values of ν = 0.25 - 0.27 have been found by measuring shear wave velocity and compression wave velocity using BE and compression piezoelectrical transducers both on the same dry specimens.

Some of the results obtained from RC tests on low density reconstituted samples, are reported in figure 5 as shear modulus normalised by its maximum value, versus shear strain. The samples were consolidated at three different isotropic pressures (i.e. p'= 100, 250 and 400 kPa). The three samples consolidated at p' = 100 kPa, show the same trend and, although there is a small difference between the G_0 values, they reflect the repeatability of the tests. Finally it can be seen that, as the pressure increases, G_0 increases and the normalised curve is shifted on the right, such that the strain level dependency of G decreases.

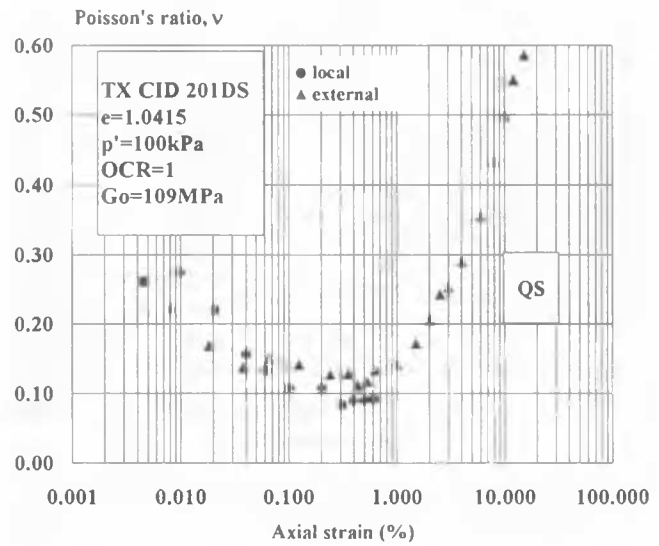

Figure 4 - Poisson's ratio versus axial strain from a TX test.

Neglecting cross coupling between shear and volumetric effects, the shear stiffness G was evaluated referring to the following relationships:

$$G = \rho V_s^2 \text{ from RC and } G = \delta q / 3\delta\varepsilon_s \text{ from TX tests}$$

where:

$V_s = 2 \pi h f / \beta$: shear wave velocity
h : height of the sample
f : resonant frequency
β : frequency factor
$q = \sigma_1 - \sigma_3$: deviatoric stress
$\varepsilon_s = 2(\varepsilon_a - \varepsilon_r)/3$: deviatoric shear strain
ε_a, ε_r: locally measured axial and radial strains respectively.

In order to obtain a more reliable value of the initial stiffness from traditional TX tests (i.e. constant cell pressure), the procedure here after reported, has been also followed:

- making the reference to the locally measured strains, the slope of the initial linear portion of the q vs. ε_a curve has been computed, obtaining the initial Young's stiffness E_0, as shown in figure 3;
- the Poisson's coefficient $\nu = -\delta\varepsilon_r/\delta\varepsilon_a$ has been evaluated from the locally axial and radial measured strains within the range of ε_a in which the Young's modulus has been assessed (see figure 4);

therefore, assuming isotropic elasticity, the shear modulus:

$$G_0 = E_0 / 2 (1+\nu).$$

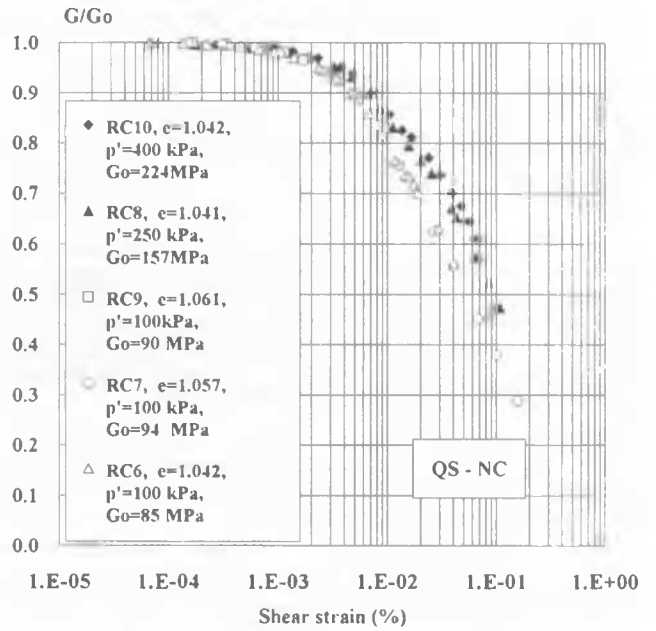

Figure 5 - Comparison of G/Go vs. shear strain relationship from RC tests.

INTERPRETATION OF THE RESULTS

The mechanical response of a geotechnical material, like QS, is generally elasto-plastic; nevertheless, it has been remarked by many researches that at very small strains ($\varepsilon < 10^{-5}$) the value of the shear modulus is practically independent of the loading conditions (i.e. static or dynamic, monotonic or cyclic) and the material shows a negligible hysteresis, therefore, from an engineering point of view, the stiffness can be assumed elastic within this range of strain (Tatsuoka and Shibuya 1991). Furthermore, the magnitude of the elastic threshold strain depends on the type of soil, on its geological and stress history, on the strain rate at which the sample is tested and on the cyclic prestrainig (e.g. Dobry and Vucetic 1987, Ampadu 1991).

As initial shear modulus, G_0, is intended the value of maximum stiffness resulting from the RC tests in the range within which it remains constant, while from TX tests the G_0 is assumed to be one third of the slope of the initial segment of the $q - \varepsilon_s$ relationship

It was established that G_0 mainly depends on state parameters such as void ratio (e) and mean effective stress (p') (Hardin and Drnevich 1972), therefore it can be expressed as:

$$G_0 = F(e)\, H(p').$$

In order to define a formulation of this functions, two assumptions are made supported by the experimental observations:

a. the shear wave velocity is linearly dependent on the void ratio, so it can be assumed:

$$F(e) = (b - e)^2/(1 + e)$$

b. the dependency of G_0 on p' can be expressed by a power function, so:

$$H(p') = p'^n.$$

In conclusion the shear modulus can be written as:

$$G_o = C_g [(b - e)^2/(1 + e)](p_r)^{(1-n)} (p')^n$$

where:

C_g = non dimensional material constant function of the soil type (multiplying C_g by F(e) one obtains the non dimensional modulus number Kg);

p_r = reference pressure = 1 MPa.

The equation that better fits the RC tests results, becomes:

$$G_o = 81.4 [(4.16 - e)^2/(1 + e)]p_r^{0.38} p'^{0.62} \qquad [G_o \text{ and } p' \text{ in MPa}].$$

In figure 6 it is reported a comparison between the above formula and all experimental data (RC, BE and TX), in terms of G_o at p' = 1 MPa versus **e** . It can be noted that all the RC tests results are located on the fitting curve within a range of ± 5 % , while for bender and triaxial tests results are more scattered for low density samples (e>0.95). The G_o values from BE are within the same range for high density samples (e < 0.9) but show generally higher values than RC and TX at medium and low density (e > 0.9).

The reasons for such a discrepancy are not easy to explain considering the theoretical frame assumed (elasticity). In first approximation, however, one can postulate that the observed difference between G_o (BE) and G_o (RC) measured might be linked to the following factors:

- difficulties in the determination of the first shear wave arrival on the receiver transducer which seems to be greater on saturated samples;
- uncertainties in the calculated Vs, due to the relatively short, few centimetres, travel path of the specimen;
- inherent difficulties in comparing different laboratory tests (the testing frequencies are different for the two tests), which is maximised because of the high sensitivity of the QS, for example to the time effects, i.e. aging during consolidation and strain rate during shearing.

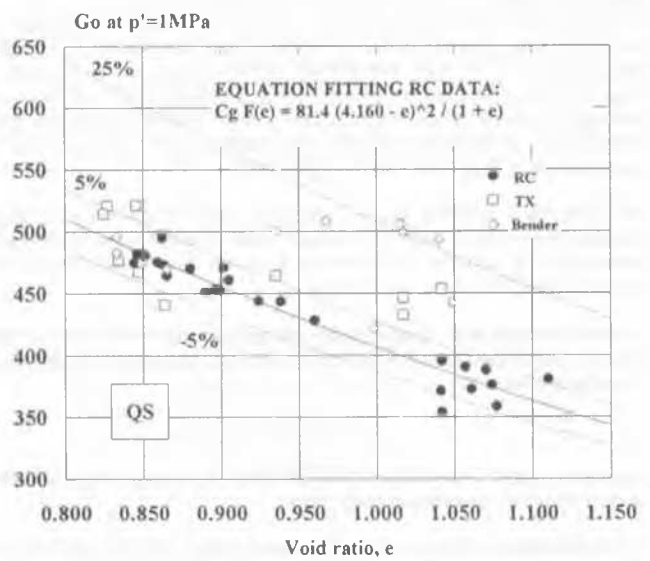

Figure 6 - Influence of e on G_o.

Effects of the overconsolidation.

The effects of the overconsolidation (OCR) on the stiffness of QS are examined on a limited number of TX tests and on 13 RC tests. In figure 7 the results of two TX tests are compared in terms of normalised secant shear modulus (G/G_o) against axial strain. Note that the elastic threshold strain becomes larger and the strain level dependency of G decreases. As the strain increases, the OCR heavily affects the secant shear modulus.

Nevertheless, contrarily to what is observed for silica sand [e.g. Tatsuoka and Shibuya (1991)], the mechanical overconsolidation seems to influence the initial shear modulus, see figure 8, where the RC tests results are reported. Since the pressure levels and the void ratios were different between NC and OC samples, the comparison was made by normalising the G_o on the G_o calculated for NC samples. The best fitting of such results gives:

$$G_o (OC) = G_o (NC) (OCR)^{0.31}$$

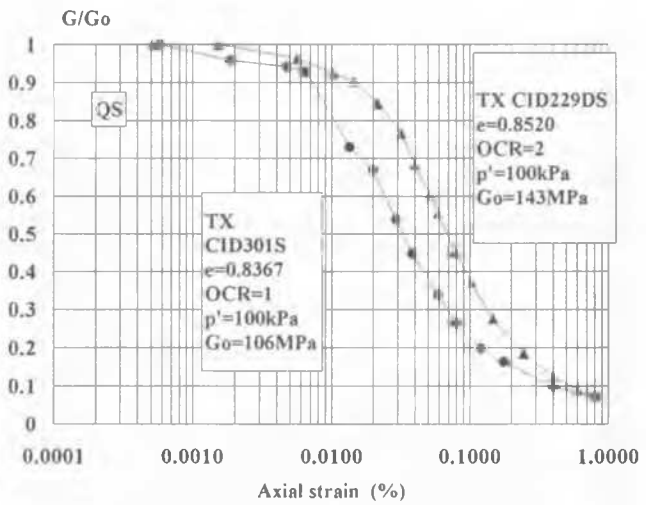

Figure 7 - Effect of OCR on G_o from TX tests.

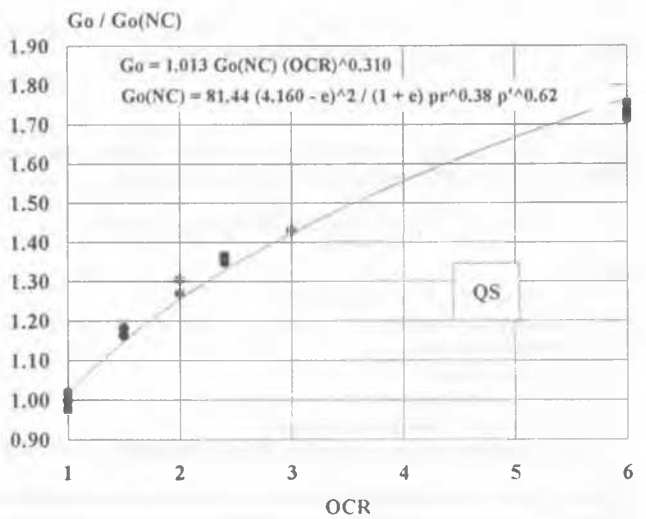

Figure 8 - Effects of OCR on G_o from RC tests.

The reasons for such behaviour is not completely clear and deserve further laboratory tests. However it can be postulated that the increasing of stress produces a crushing of the particles and their rearrangement, with consequent increase of the number of inter-particle contacts. Upon unloading, the recoverable deformation is so low that the number of inter-particle contacts remains almost unchanged and appreciably higher than those of a virgin sample at the same p'. The effect of crushing apparently is not adequately reflected in the actual void ratio function.

The influence of soil non-linearity and OCR on modelling stress-strain response of soils is evidentiated in figure 9, which shows the ratio of q/q_{max} (TX) and τ/τ_{max}(RC) on the horizontal axis versus the ratio E/E_0 (TX) and G/G_0 (RC) on the vertical axis.

Both E and G correspond to the secant deformation moduli, the diagonal line shown in figure 9 reflects the hyperbolic stress-strain relationship. It is clear that the NC exhibits a non linearity much higher than the one that can be obtained by the hyperbolic stress-strain model. As the OCR increases, the stress strain curves moves closer to the hyperbola which better fits the data from RC tests; for similar results see Tatsuoka and Shibuya (1991) and Jamiolkowski et al. (1991).

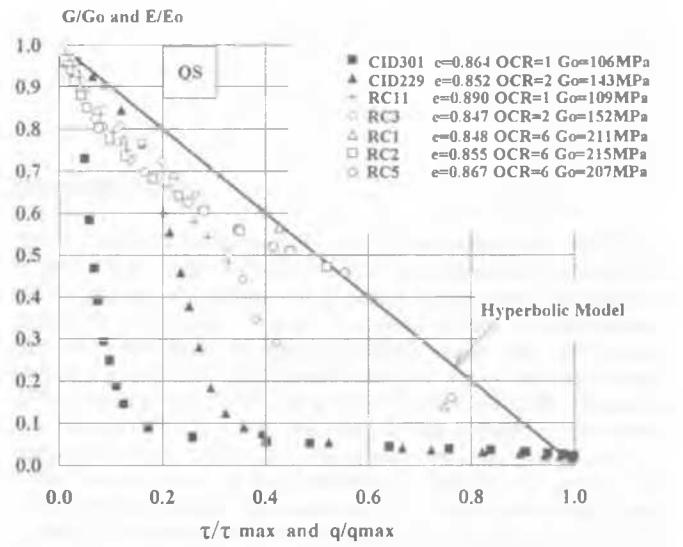

Figure 9 - Normalised secant shear and Young moduli versus shear stress level.

CLOSING REMARKS

1 Local measurements of axial and radial deformations in a TX test are suggested to obtain more reliable data, to increase the precision in measuring stiffness at very small strains, so the data can be compared to other tests (RC and BE).

2 For NC samples, the maximum shear modulus G_0, depends principally on the state parameters: void ratio and mean effective stress. For practical purposes by fitting the experimental data, a similar expression can be found:

$$G_0 = F(e)\, H(p') = 81.4\, [(4.16 - e)^2/(1 + e)]\, p_r^{0.38}\, p'^{0.62}$$

The increase of the consolidation pressure has the effect of decreasing the strain level dependency of the shear modulus.

3 Similar magnitudes of the initial stiffness at comparable void ratio have been found from RC and TX tests, while G_0 values from BE are generally 20 % greater at low density. More tests are required in this direction.

4 When QS is strained beyond the elastic threshold, its stress-strain response appears highly non linear.

5 The effects of the OCR on QS can be summarised as follows:

increasing the elastic threshold
decreasing the strain level dependency of G
increasing the maximum value of the shear modulus.

6 Assuming E_0 or G_0 to be the initial stiffness of QS the hyperbolic model does not fit their stress-strain curve. Nevertheless, results from RC tests and generally for samples with high OCR, seem to be closer to the hyperbolic relationship.

ACKNOWLEDGEMENTS

All the tests presented in this paper were performed at ISMES: The authors would like to thank Mr. O. Hameury for the execution of the RC tests and for being involved in the interpretation analysis of the results; Mr R. Capoferri for the execution of the triaxial tests and for the support given.

REFERENCES

Almeida, M. S. S., Jamiolkowski, M. and Peterson R. W. (1991). *Preliminary results of CPT tests in calcareous Quiou Sand.* First International Symp. on CC Testing ISOCCT-1. Potsdam.

Ampadu, S. I. K. (1991). *Undrained behaviour of kaolin in torsional simple shear.* Ph.D. thesis, University of Tokyo.

Baldi, G., Fretti, C., Lo Presti, D. C. F. and Salgado, R.(1991). *Research dilatometer: In situ and Chamber Calibration results.* ISOCCT-1 Potsdam.

Bellotti, R., Bizzi G. and Ghionna, V. N. (1982). *Design, construction and use of a Calibation Chamber.* Pore. ESOPT II. Amsterdam.

Bellotti, R. et al. (1988). *Saturation of sand specimens for calibration chamber tests.* Proc. ISOPT-1 Orlando, Fla.

Bellotti, R., Fretti, C., Ghionna, V. N. and Pedroni, S. (1991). *Crushability of sands in CPT performed in Calibration Chamber.* Proc. 9-th ARC on SMFE, Bangkok.

Brignoli, E. and Gotti, M. (1992). *Misure di velocita' di onde di taglio in laboratorio con l'impiego di trasduttori piezoelettrici.* Rivista Italiana di Geotecnica. XXVI n.1.

Dobry, R. and Vucetic, M. (1987). State-of-the Art report: *Dynamic properties and response of soft clay deposits.* Proc. Intl. Symposium on Geotechnical Eng. of Soft Soils, Mexico City.

Jamiolkowski, M., Le Roueil, S. and Lo Presti, D. C. F. (1991). *Design parameters from theory to practice.* Team Lecture. Geo-Coast'91. Yokohama.

Passalacqua, R., (1991). *A sand spreader used for the reconstitution of granular soil models.* Soils and Foundations, JSSMFE, Vol.31, n.2, pp. 175,180.

Shibuya, S., Tatsuoka, F., Teachavorasinsekun, S., Kong. X.J., Abe, F., Kim, Y.S. and Pask, C. S., (1992). *Elastic Deformation Properties on Geomaterials.* Soils and Foundations, n. 3.

Tatsuoka, F. and Shibuya, S.(1991). *Deformation characteristics of soil and Rocks from Field and Laboratory tests.* Proc. 9-th ARC on SMFE, Bangkok.